An Iterative Algorithm Between Stream Function and Density for Transonic Cascade Flow

Bao-Guo Wang*
Chinese Academy of Sciences, Institute of Engineering Thermophysics, Beijing, China

A set of Wu's equations governing the fluid flow along a given S_1 stream surface is solved by the use of artificial compressibility and a new iterative algorithm between the two variables stream function ψ and density ρ. The set of equations consists of a stream function equation and a new first-order partial differential equation for density derived from the continuity equation, momentum equation and Bernoulli's equation. The stream function equation proposed by Wu more than 30 years ago is written in general curvilinear coordinate system to allow for arbitrary boundary shapes. A strongly implicit approximate factorization algorithm (SI) of the multidimensional partial differential equations is used in numerical solutions of this set of equations. By the method proposed in this paper, the problem of nonuniqueness of density in the conventional stream function method is avoided. A number of transonic cascades are calculated and given herein to demonstrate the capability of the present method.

I. Introduction

In order to discretize the mixed-type full potential equation or stream function equation in a transonic flowfield, the artificial compressibility method[1] could be considered. This method consists of modifying the density in such a way as to introduce the numerical dissipation necessary in the supersonic region. With a slight modification of the density in the supersonic region, the transonic flow problem becomes amenable to treatment by standard discretization techniques (central differencing) and some standard iterative procedures (SOR, ADI, explicit methods, and implicit algorithms[2-12]). The approximate factorization schemes, for example AF1, AF2, AF3, and SI, can be used to solve the conservative or nonconservative transonic full-potential equation[3-5,7-9,12] and transonic stream function equation.[2,6,10,11] For transonic flows, this scheme has proved to be fast and reliable and, therefore, is the only scheme considered in this study.

For transonic cascade flow, the irrotational assumption is not valid when the entropy is nonuniform downstream of a strong shock. Without the assumption of uniform entropy or irrotational flow, the stream function equation is more suitable. However, the main difficulty with the solution of stream function in transonic flow lies in that the density is not uniquely determined in terms of mass flux. The purpose of this study is to develop efficient algorithm to overcome this difficulty.

In the present paper, a set of Wu's equations[13-16] governing the fluid flow along S_1 surface is solved by the combination of the artificial compressibility and a new iterative algorithm between the two variables ψ and ρ. The set of equations consists of a stream function equation and a new first-order partial differential equation for density derived from continuity equation, momentum equation, and Bernoulli's equation. The SI algorithm is used in the numerical solutions of this set of equations. The problem of nonuniqueness of density in traditional stream function method is avoided in this study.

Received April 22, 1985; revision received Dec. 24, 1985.

*Research Scientist, Applied Computational Thermophysics Branch.

II. Stream Function Equation on S_1 Surface

The governing equations for the steady relative flow of a nonviscous fluid on S_1 stream surface are[14,15]

$$\frac{\partial}{\partial x^2}[(W^1+W^2\cos\theta_{12})\sqrt{g_{11}}]-\frac{\partial}{\partial x^1}[(W^1\cos\theta_{12}+W^2)\sqrt{g_{22}}]$$
$$=2\sqrt{g}\omega^3+\frac{\sqrt{g_{11}}}{W^1}\left(\frac{\partial I}{\partial x^2}-T\frac{\partial S}{\partial x^2}\right) \tag{1}$$

where W^1 and W^2 denote physical components of relative velocity in X^1 and X^2 directions. By using definition of the stream function based on the continuity equation, Eq. (1) can be rearranged into the following form[16]

$$\frac{\partial}{\partial x^1}\left(\frac{A_{21}}{\rho}\frac{\partial\psi}{\partial x^1}+\frac{A}{\rho}\frac{\partial\psi}{\partial x^2}\right)$$
$$+\frac{\partial}{\partial x^2}\left(\frac{A_{12}}{\rho}\frac{\partial\psi}{\partial x^2}+\frac{A}{\rho}\frac{\partial\psi}{\partial x^1}\right)=D \tag{2a}$$

or

$$\frac{A_{21}}{\rho}\frac{\partial^2\psi}{\partial(x^1)^2}+2\frac{A}{\rho}\frac{\partial^2\psi}{\partial x^1\partial x^2}+\frac{A_{12}}{\rho}\frac{\partial^2\psi}{\partial(x^2)^2}$$
$$+\left[\frac{\partial}{\partial x^1}\left(\frac{A_{21}}{\rho}\right)+\frac{\partial}{\partial x^2}\left(\frac{A}{\rho}\right)\right]\frac{\partial\psi}{\partial x^1}$$
$$+\left[\frac{\partial}{\partial x^1}\left(\frac{A}{\rho}\right)+\frac{\partial}{\partial x^2}\left(\frac{A_{12}}{\rho}\right)\right]\frac{\partial\psi}{\partial x^2}=D \tag{2b}$$

where

$$\frac{\partial\psi}{\partial x^1}=-\tau\rho\sqrt{g_{11}}W^2\sin\theta_{12} \tag{3}$$

$$\frac{\partial\psi}{\partial x^2}=\tau\rho\sqrt{g_{22}}W^1\sin\theta_{12} \tag{4}$$

g_{11} and g_{22} are the metric tensor of x^i coordinate system, τ is the thickness of S_1 stream filament, and θ_{12} is the angle between coordinate lines x^1 and x^2. It can be shown that Eqs. (2a) or (2b) is a mixed-type equation, that is, in subsonic region, it is an elliptic equation, but in supersonic regions, it is a hyperbolic equation. In order to introduce the necessary

artificial viscosity to ensure uniqueness of the difference equations and the capture of the shockwave, the density in Eq. (2a) should be replaced by a corresponding artificial density $\tilde{\rho}$. The formula for calculating artificial density is

$$\tilde{\rho} \approx \rho - \nu[(W^1/W)\Delta x^1 \overleftarrow{\delta}_{x1}\rho + (W^2/W)\Delta x^2 \overrightleftarrows{\delta}_{x2}\rho] \tag{5}$$

or

$$\begin{aligned}\tilde{\rho}_{j,i} \approx \rho_{j,i} - \nu_{j,i}\{&(W^1/W)_{j,i}(\rho_{j,i}-\rho_{j,i-1}) \\ &+ \tfrac{1}{2}(W^2/W)_{j,i}[(\rho_{j+1,i}-\rho_{j-1,i}) \\ &- \text{sign}(1, W^2)(\rho_{j+1,i}-2\rho_{j,i}+\rho_{j-1,i})]\}\end{aligned} \tag{6}$$

where

$$\left.\begin{aligned} \nu_{j,i} &= \max[0,\ C_0(1-1/M_{j,i}^2)] \\ \Delta x^1 \overleftarrow{\delta}_{x1}\rho &= \rho_{j,i}-\rho_{j,i-1} \\ \Delta x^2 \overrightleftarrows{\delta}_{x2}\rho &= \begin{cases} \rho_{j,i}-\rho_{j-1,i} & (W_{j,i}^2>0) \\ \rho_{j+1,i}-\rho_{j,i} & (W_{j,i}^2<0) \end{cases} \end{aligned}\right\} \tag{7}$$

C_0 is a user-specified constant in the range of $0.5\sim3$ and $M_{j,i}$ is relative flow Mach number at (j,i). The double arrow in the superscript means that when $W^2>0$, $\overleftarrow{\delta}_{x2}$ is selected, and when $W^2<0$, $\overrightarrow{\delta}_{x2}$ is selected. In a nonorthogonal coordinate system the artificial density specified by Eq. (5) is similar in the form to $\tilde{\rho}$ given by Ref. 4. Therefore, the principal equation in stream function can be written in the following form[6]:

$$\frac{\partial}{\partial x^1}\left(\frac{A_{21}}{\tilde{\rho}}\frac{\partial\psi}{\partial x^1}+\frac{A}{\tilde{\rho}}\frac{\partial\psi}{\partial x^2}\right)+\frac{\partial}{\partial x^2}\left(\frac{A_{12}}{\tilde{\rho}}\frac{\partial\psi}{\partial x^2}+\frac{A}{\tilde{\rho}}\frac{\partial\psi}{\partial x^1}\right)=D \tag{8}$$

where

$$A=-\left(\tau\frac{\sin\theta_{12}}{\cos\theta_{12}}\right)^{-1}, \qquad A_{12}=\sqrt{g_{11}/g_{22}}(\tau\sin\theta_{12})^{-1}$$

$$A_{21}=\sqrt{g_{22}/g_{11}}(\tau\sin\theta_{12})^{-1}$$

$$D=2\sqrt{g}\omega^3+\frac{\sqrt{g_{11}}}{W^1}\left(\frac{\partial I}{\partial x^2}-T\frac{\partial S}{\partial x^2}\right)$$

It is seen that the entropy appears in Eq. (8). The entropy increase across the shock is evaluated from the following equations[17]:

$$\begin{aligned}\frac{S_2-S_1}{R}=&\frac{K}{K-1}\ell n\left[\frac{2}{(K+1)M_1^2\sin^2\sigma}+\frac{K-1}{K+1}\right] \\ &+\frac{1}{K-1}\ell n\left[\frac{2K}{K+1}M_1^2\sin^2\sigma-\frac{K-1}{K+1}\right]\end{aligned} \tag{9}$$

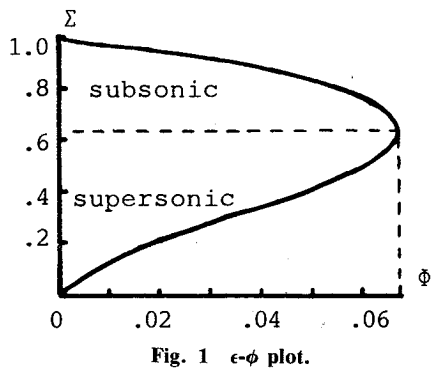

Fig. 1 ϵ-ϕ plot.

where M is the Mach number of the flow and σ the shock angle, R is the universal gas constant, and K is the ratio of specific heats. In the preceding expression, the subscripts 1 and 2 represent the upstream and downstream of the shock, respectively.

III. Difference Scheme and SI Procedure

Standard finite differences are used in discretizing Eq. (8), i.e., central differencing everywhere, leading to a large system of nonlinear algebraic equations in the unknown stream function values at the grid points. A second-order-accurate finite difference approximation to Eq. (8) is given by[2,6]

$$\begin{aligned}L\psi_{j,i} = &\overleftarrow{\delta}_{x1}\{[(A_{21}/\tilde{\rho})\delta_{x1}+(A/\tilde{\rho})\delta_{x2}]\psi\}_{j,i+\frac{1}{2}} \\ &+\overleftarrow{\delta}_{x2}\{[(A_{12}/\tilde{\rho})\delta_{x2}+(A/\tilde{\rho})\delta_{x1}]\psi\}_{j+\frac{1}{2},i} \\ &=2(\sqrt{g}\omega^3)_{j,i}+(\sqrt{g_{11}}/W^1)_{j,i}[(I_{j+1,i}-I_{j-1,i}) \\ &-T_{j,i}(S_{j+1,i}-S_{j-1,i})]/(2\Delta x^2)=D_{j,i}\end{aligned} \tag{10}$$

where

$$\delta_{x1}(\ )_{j,i+\frac{1}{2}}=[(\ )_{j,i+1}-(\ )_{j,i}]/\Delta x^1$$

$$\delta_{x2}(\ )_{j+\frac{1}{2},i}=[(\ )_{j+1,i}-(\ )_{j,i}]/\Delta x^2$$

$$\delta_{x1}(\ )_{j+\frac{1}{2},i}=[(\ )_{j+1,i+1}-(\ )_{j+1,i-1}+(\ )_{j,i+1}-(\ )_{j,i-1}]/(4\Delta x^1)$$

$$\delta_{x2}(\ )_{j,i+\frac{1}{2}}=[(\ )_{j+1,i+1}-(\ )_{j-1,i+1}+(\ )_{j+1,i}-(\ )_{j-1,i}]/(4\Delta x^2)$$

$$\overleftarrow{\delta}_{x1}(\ )_{j,i+\frac{1}{2}}=[(\ )_{j,i+\frac{1}{2}}-(\ )_{j,i-\frac{1}{2}}]/\Delta x^1$$

$$\overleftarrow{\delta}_{x2}(\ )_{j+\frac{1}{2},i}=[(\ )_{j+\frac{1}{2},i}-(\ )_{j-\frac{1}{2},i}]/\Delta x^2$$

The spatially differenced quantities in Eq. (10) are evaluated at computational grid half-points. All the quantities at half-points were treated as the mean value of the two neighboring grid points. Thus, the computational module for this expression is a nine-point star which includes contributions from grid points identified by the indices $(j-1,i-1)$, $(j-1,i)$, $(j-1,i+1)$, $(j,i-1)$, (j,i), $(j,i+1)$, $(j+1,i-1)$, $(j+1,i)$, and $(j+1,i+1)$. At each interior point (j,i), Eq. (10) can be put in compact form as follows:

$$\begin{aligned}&B_{1j,i}\psi_{j,i-1}+B_{2j,i}\psi_{j,i}+B_{3j,i}\psi_{j,i+1}+B_{4j,i}\psi_{j-1,i-1}+B_{5j,i}\psi_{j-1,i} \\ &+B_{6j,i}\psi_{j-1,i+1}+B_{7j,i}\psi_{j+1,i-1}+B_{8j,i}\psi_{j+1,i}+B_{9j,i}\psi_{j+1,i+1}=D_{j,i}\end{aligned}$$

or (11a)

$$B_{1j,i}\psi_{j,i-1}+B_{2j,i}\psi_{j,i}+B_{3j,i}\psi_{j,i+1}+B_{5j,i}\psi_{j-1,i}+B_{8j,i}\psi_{j+1,i}=\bar{P}_{j,i} \tag{11b}$$

where

$$\begin{aligned}\bar{P}_{j,i}=&D_{j,i}-B_{4j,i}\psi_{j-1,i-1}-B_{6j,i}\psi_{j-1,i+1} \\ &-B_{7j,i}\psi_{j+1,i-1}-B_{9j,i}\psi_{j+1,i+1}\end{aligned}$$

Equation (11b) can also be written, like AF and ADI schemes, before factorization as

$$[\bar{M}]^{(n)}\{\psi\}^{(n+1)}=\{\bar{P}\}^{(n)} \tag{12}$$

or

$$[\bar{M}]^{(n)}\{\xi\}^{(n+1)}=\{R\}^{(n)} \tag{13}$$

where { } represents column matrix, and $\{\bar{p}\}$, $\{R\}$, and $\{\xi\}$ are in terms of ψ and ρ at each grid point and $[\bar{M}]^{(n)}$ is the matrix composed of the coefficients for the nth iterative level. $\xi^{(n+1)} \equiv \psi^{(n+1)} - \psi^{(n)}$ and $\{R\}^{(n)}$ is the residual at iteration level n. The (j,i)th element of $\{R\}^{(n)}$ is defined by

$$R_{j,i}^{(n)} \equiv D_{j,i}^{(n)} - L\psi_{j,i}^{(n)} = R(\psi^{(n)})_{j,i} \tag{14}$$

or

$$\{R\}^{(n)} = \{\bar{P}\}^{(n)} - [\bar{M}]^{(n)}\{\psi\}^{(n)} \tag{15}$$

where the coefficient matrix $[\bar{M}]^{(n)}$ is a function of $\bar{\rho}$. It is convenient to use the notation of Eq. (11b) in $[\bar{M}]^{(n)}$, so that each row of this matrix contains at most five nonzero elements; these are $B_{1j,i}$, $B_{2j,i}$, $B_{3j,i}$, $B_{5j,i}$, and $B_{8j,i}$. It is important to note that this notation does not conform to the standard matrix notation; the subscripts (j,i) refer to the grid system used in setting up the difference equations, rather than the location within the matrix.

At each interior point, Eq. (13) can be formally written as

$$B_{1j,i}^{(n)}\xi_{j,i-1}^{(n+1)} + B_{2j,i}^{(n)}\xi_{j,i}^{(n+1)} + B_{3j,i}^{(n)}\xi_{j,i+1}^{(n+1)} + B_{5j,i}^{(n)}\xi_{j-1,i}^{(n+1)} + B_{8j,i}^{(n)}\xi_{j+1,i}^{(n+1)} = R_{j,i}^{(n)} \tag{16}$$

In order to solve Eq. (16), the SI algorithm proposed by Stone[18] is used. It is to transform the matrix $[\bar{M}]$ into a seven-diagonal matrix $[M]$ by appending certain second-order error terms which allow a simple factorization into sparse-banded $[L]$ and $[U]$ matrices. In the present paper, it is accomplished by adding the following error terms to the left-hand side of Eq. (16):

$$B_{6j,i}^{(n)}[\xi_{j-1,i+1}^{(n+1)} - \alpha(\xi_{j-1,i}^{(n+1)} + \xi_{j,i+1}^{(n+1)} - \xi_{j,i}^{(n+1)})] + B_{7j,i}^{(n)}[\xi_{j+1,i-1}^{(n+1)} - \alpha(\xi_{j,i-1}^{(n+1)} + \xi_{j+1,i}^{(n+1)} - \xi_{j,i}^{(n+1)})]$$

Here, α is a sequence of constants given by

$$\alpha_\ell = \alpha_m(\alpha_n/\alpha_m)^{\ell/(\bar{N}-1)} \qquad (\ell = 0,1,2,\ldots,\bar{N}-1) \tag{17}$$

The ranges of α_m and α_n are $7 \sim 12$ and $0.75 \sim 1.5$, respectively. $\bar{N}$ is an integer and its value is 9 in this study. If the above error terms are added to Eq. (16), the resulting expression takes on the following factored form:

$$(a_{j,i}^{(n)}E_{x1}^{-} + b_{j,i}^{(n)}E_{x2}^{-} + C_{j,i}^{(n)})(1 + d_{j,i}^{(n)}E_{x2}^{+} + e_{j,i}^{(n)}E_{x1}^{+})\xi_{j,i}^{(n+1)} = R_{j,i}^{(n)} \tag{18}$$

where E_{x1}^{-}, E_{x2}^{+}, etc. are the usual shift operators:

$$E_{x1}^{\pm}\xi_{j,i}^{(n+1)} \equiv \xi_{j,i\pm1}^{(n+1)}, \qquad E_{x2}^{\pm}\xi_{j,i}^{(n+1)} \equiv \xi_{j\pm1,i}^{(n+1)}$$

The coefficients $a_{j,i}^{(n)}$, $b_{j,i}^{(n)}$, etc. may be determined by the following relationships

$$a_{j,i}^{(n)} = B_{1j,i}^{(n)}/[1 + \alpha d_{j,i-1}^{(n)}] \tag{19a}$$

$$b_{j,i}^{(n)} = B_{5j,i}^{(n)}/[1 + \alpha e_{j-1,i}^{(n)}] \tag{19b}$$

$$c_{j,i}^{(n)} = B_{2j,i}^{(n)} + (\alpha e_{j-1,i}^{(n)} - d_{j-1,i}^{(n)})b_{j,i}^{(n)} + (\alpha d_{j,i-1}^{(n)} - e_{j,i-1}^{(n)})a_{j,i}^{(n)} \tag{19c}$$

$$d_{j,i}^{(n)} = (B_{8j,i}^{(n)} - \alpha a_{j,i}^{(n)}d_{j,i-1}^{(n)})/c_{j,i}^{(n)} \tag{19d}$$

$$e_{j,i}^{(n)} = (B_{3j,i}^{(n)} - \alpha b_{j,i}^{(n)}e_{j-1,i}^{(n)})/c_{j,i}^{(n)} \tag{19e}$$

Equations (19) are actually used in the computation. In order to close the system, the quantities $a_{j,i}^{(n)}$, $b_{j,i}^{(n)}$, etc., are set to zero at all the boundaries.

Implementation of the SI scheme is achieved by writing it in a two-step form given by:

Step 1:

$$f_{j,i}^{(n)} = [R_{j,i}^{(n)} - a_{j,i}^{(n)}f_{j,i-1}^{(n)} - b_{j,i}^{(n)}f_{j-1,i}^{(n)}]/c_{j,i}^{(n)} \tag{20}$$

Step 2:

$$\xi_{j,i}^{(n+1)} = f_{j,i}^{(n)} - d_{j,i}^{(n)}\xi_{j+1,i}^{(n+1)} - e_{j,i}^{(n)}\xi_{j,i+1}^{(n+1)} \tag{21}$$

where $f_{j,i}^{(n)}$ is an intermediate result stored at each mesh point. In order to close the system, the quantities $f_{j,i}^{(n)}$ and $\xi_{j,i}^{(n)}$ are also set to zero at all the boundaries.

In the present investigation, the periodicity boundary condition is specified by the following equations:

$$\psi_{1,i}^{(n+1)} = 1/6[4(\psi_{2,i}^{(n+1)} + \psi_{N-1,i}^{(n+1)}) - (\psi_{3,i}^{(n+1)} + \psi_{N-2,i}^{(n+1)}) - 3G] \tag{22}$$

$$\psi_{N,i}^{(n+1)} = \psi_{1,i}^{(n+1)} + G \tag{23}$$

where subscript $N \equiv j_{\max}$ and G denotes mass flow. Note that Eqs. (22) and (23) are derived from the following relationships:

$$\psi_{N,i} - \psi_{1,i} = G, \qquad W_{N,i}^{1} = W_{1,i}^{1}$$

Here W^1 is physical component of relative velocity along the X^1 direction.

IV. The Velocity Gradient Method

The density-mass flow relation is as follows:

$$\rho/\rho_i = \left\{\left[I + \frac{1}{2}(\omega\gamma)^2 - \frac{1}{2}\frac{(\rho W)^2}{\rho^2}\right]\Big/h_i\right\}^{1/(K-1)} e^{-\Delta S/R} \tag{24}$$

where I is the relative stagnation rothalpy of unit mass of gas, $I \equiv h - (U^2/2) + [(W)^2/2]$; ρ_i is the density, and h_i is the enthalpy at inlet station. The entropy increment ΔS is defined as $\Delta S \equiv S - S_i$. Equation (24) can be rewritten as [see Eq. (39) in Ref. 16]:

$$\Sigma^2 = \left(1 - \frac{\Phi}{\Sigma^2}\right)^{2/(K-1)} \tag{25}$$

where Σ is a function of ρ and Φ is a function of ρW. The Σ-Φ plot, which contains the subsonic and supersonic branches (see Fig. 1), indicates that there are two values of density for a certain value of mass flow.

Equation (24) can be rewritten as:

$$F(\rho) \equiv h_i[(e^{\Delta S/R})/\rho_i]^{K-1}\rho^{K+1} - [I + \tfrac{1}{2}(\omega\gamma)^2]\rho^2 + \frac{1}{2}\left[\left(\frac{1}{\tau\sqrt{g_{22}}\sin\theta_{12}}\frac{\partial\psi}{\partial x^2}\right)^2 + \left(\frac{1}{\tau\sqrt{g_{11}}\sin\theta_{12}}\frac{\partial\psi}{\partial x^1}\right)^2 - 2\frac{\partial\psi}{\partial x^1}\frac{\partial\psi}{\partial x^2}\left(\frac{1}{\tau\sin\theta_{12}}\right)^2\frac{\cos\theta_{12}}{\sqrt{g_{11}}\sqrt{g_{22}}}\right] = 0 \tag{26}$$

For pure subsonic or pure supersonic flows Newton's iteration to Eq. (26) may be used. But for transonic flow, perturbing sonic conditions yields two possible solutions, and it is not obvious which one has to be chosen. To avoid the ambiguity in the density updating, a useful approach is suggested in Ref. (2), namely to calculate the velocity from the momentum equation. Once W is known, the density is updated through Bernoulli's equation as before. The momentum equation can be expressed in the form of velocity gradient and the corresponding velocity gradient equation for

transonic cascade flow is[19]

$$\frac{\partial}{\partial x^2}(C_2 W^1) = D - \frac{\partial}{\partial x^1}(C_1) \tag{27}$$

where

$$C_1 = \sqrt{g_{22}}\left[\left(\frac{\partial\psi}{\partial x^1}\right)(\sqrt{g_{22}}/\sqrt{g_{11}})\Big/\left(\frac{\partial\psi}{\partial x^2}\right) - \cos\theta_{12}\right] \times \left(\frac{\partial\psi}{\partial x^2}\right)\Big/(\tau\tilde{\rho}\sqrt{g_{22}}\sin\theta_{12})$$

$$C_2 = \sqrt{g_{11}}\left[1 - \left(\frac{\partial\psi}{\partial x^1}\right)(\sqrt{g_{22}}/\sqrt{g_{11}})(\cos\theta_{12})\Big/\left(\frac{\partial\psi}{\partial x^2}\right)\right]$$

After W^1 is, thus, updated, W^2, W, and ρ are obtained from the following relations:

$$W^2 = -\frac{\partial\psi/\partial x^1}{\partial\psi/\partial x^2}\sqrt{\frac{g_{22}}{g_{11}}}\,W^1 \tag{28}$$

$$W = [(W^1)^2 + (W^2)^2 + 2W^1W^2\cos\theta_{12}]^{1/2} \tag{29}$$

$$\frac{\rho}{\rho_i} = \left[\frac{I + \tfrac{1}{2}(\omega\gamma)^2 - \tfrac{1}{2}(W)^2}{h_i}\right]^{1/(K-1)} e^{-\Delta S/R} \tag{30}$$

V. New Equation for Density

The basic aerothermodynamic equations governing the steady relative flow of an inviscid gas are[13]

$$\nabla\cdot(\rho\vec{W}) = 0 \tag{31}$$

$$\frac{\mathrm{d}'\vec{W}}{\mathrm{d}t} - (\omega)^2\vec{\gamma} + 2\vec{\omega}\times\vec{W} = -\frac{\nabla p}{\rho} \tag{32}$$

$$\frac{(W)^2 - (\omega\gamma)^2}{2} + \int\frac{\mathrm{d}p}{\rho} = \text{const (along streamline)} \tag{33}$$

Equation (31) is multiplied by $(W^1\cos\theta_{12} + W^2)\sqrt{g_{22}}$, the dot product of Eq. (32) with $\tau\rho\sqrt{g}\vec{e_2}$ is taken and the results are added to get, with aid of Eq. (33),

$$\frac{\partial}{\partial x^1}(C_3/\rho) + \frac{\partial}{\partial x^2}(C_4/\rho) + (C_5/\rho) = C_6 \tag{34}$$

where

$$C_3 = \left(g_{12}\frac{\partial\psi}{\partial x^2} - g_{22}\frac{\partial\psi}{\partial x^1}\right)\frac{\partial\psi}{\partial x^2}(\tau\sqrt{g})^{-1}$$

$$C_4 = \left(g_{22}\frac{\partial\psi}{\partial x^1} - g_{12}\frac{\partial\psi}{\partial x^2}\right)\frac{\partial\psi}{\partial x^1}(\tau\sqrt{g})^{-1} - \frac{K-1}{2K}(\tau)^{-1} \times\sqrt{g}\left(g^{11}\frac{\partial\psi}{\partial x^1}\frac{\partial\psi}{\partial x^1} + 2g^{12}\frac{\partial\psi}{\partial x^1}\frac{\partial\psi}{\partial x^2} + g^{22}\frac{\partial\psi}{\partial x^2}\frac{\partial\psi}{\partial x^2}\right)$$

$$C_5 = \left[\left(g_{11}\frac{\partial\psi}{\partial x^2} - g_{12}\frac{\partial\psi}{\partial x^1}\right)\left(\Gamma^1_{22}\frac{\partial\psi}{\partial x^1} - \Gamma^1_{12}\frac{\partial\psi}{\partial x^2}\right) + \left(g_{12}\frac{\partial\psi}{\partial x^2} - g_{22}\frac{\partial\psi}{\partial x^1}\right)\left(\Gamma^2_{22}\frac{\partial\psi}{\partial x^1} - \Gamma^2_{12}\frac{\partial\psi}{\partial x^2}\right)\right](\tau\sqrt{g})^{-1}$$

$$C_6 = -2\omega^3\sqrt{g}\frac{\partial\psi}{\partial x^2} + p\frac{\partial}{\partial x^2}(\tau\sqrt{g}) - \frac{\partial}{\partial x^2}\left\{\frac{K-1}{K}\tau\sqrt{g}[C_7 + \tfrac{1}{2}(\omega\gamma)^2]\rho\right\} + \left[\tau\sqrt{g}(\omega)^2\gamma\frac{\partial}{\partial x^2}(\gamma)\right]\rho$$

$$\Gamma^m_{ij} = \frac{1}{2}\left(\frac{\partial g_{ki}}{\partial x^j} + \frac{\partial g_{kj}}{\partial x^i} - \frac{\partial g_{ij}}{\partial x^k}\right)g^{km}$$

The quantities Γ^k_{ij} are called Christoffel symbols of the second kind; r and τ, radius of stream surface of revolution and thickness of stream sheet; and p, pressure. By using Bernouilli's equation along any relative streamline, p may be obtained as

$$p = \frac{K-1}{K}\{C_7\rho - [\tfrac{1}{2}(W)^2 - \tfrac{1}{2}(\omega\gamma)^2]\rho\} \tag{35}$$

Here

$$C_7 \equiv \frac{K}{K-1}\left(\frac{p}{\rho}\right)_i + [\tfrac{1}{2}(W)^2 - \tfrac{1}{2}(\omega\gamma)^2]_i$$

In the preceding expression subscript i expresses inlet.

For plane cascade r=const, τ=const and $\omega=0$, and in Cartesian coordinates Eq. (34) becomes

$$\frac{\partial}{\partial x}\left[\frac{(\nabla\psi)\cdot(\nabla\psi)\sin\theta\cos\theta}{\rho}\right] + \frac{\partial}{\partial y}\left[\frac{(\nabla\psi)\cdot(\nabla\psi)(\sin^2\theta - [(K-1)/2K])}{\rho} + C_8\right] = 0 \tag{36a}$$

or

$$\frac{\partial}{\partial x}(\rho uv) + \frac{\partial}{\partial y}(\rho vv + p) = 0 \tag{36b}$$

where (x,y) denote the distance along and perpendicular to the axis and (u,v) the velocity components in these direction; $\nabla\psi$ denotes the gradient of ψ; and

$$tg\theta = \frac{v}{u} = -\left(\frac{\partial\psi}{\partial x}\right)\Big/\left(\frac{\partial\psi}{\partial y}\right), \quad C_8 \equiv (K-1/K)C_7\rho$$

Equation (36b) is similar in form to Eq. (36) of Ref. 2.

It is important to note that Eq. (34) or (36a) is a new first-order partial differential equation for density. This equation

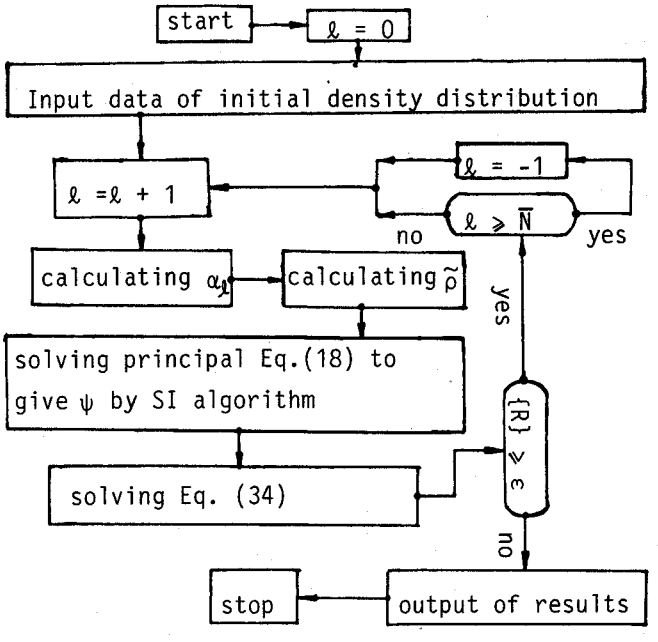

Fig. 2 Flowchart of sequence of calculations.

can easily be solved by using SI algorithm and central differencing[20] everywhere for ρ at the grid points. This idea is adopted in the present paper.

Equation (34) can also be rearranged into the following form:

$$\frac{\partial}{\partial x^1}(C_3/\rho)+C_5/\rho=C_6-\frac{\partial}{\partial x^2}(C_4/\rho) \tag{37}$$

or

$$\frac{\partial}{\partial x^2}(C_4/\rho)+C_5/\rho=C_6-\frac{\partial}{\partial x^1}(C_3/\rho) \tag{38}$$

Once these terms on the right-hand side of Eqs. (37) and (38) are obtained in the preceding cycle, Eq. (37) or (38) may be easily solved by using integration along X^1 or X^2 direction. The idea is adopted for the current investigation, also.

VI. Flowchart of the Numerical Scheme

For the present calculation a flowchart depicting the complete sequence of calculations (Fig. 2) is shown below.

In the previous calculation, it should be mentioned that the entropy increase across the shock is calculated in terms of the Mach number upstream of the shock and the shock angle. The entropy along a streamline downstream of the shock remains constant.

VII. Numerical Results

In order to investigate the possibility of determining the density field by using Eq. (34) or (36a), a number of transonic cascades have been calculated. The first test example is the computation of the Hobson cascade[21] carried out on a 50×11 mesh, inlet Mach number of 0.575, both the inlet and outlet angles are 46.1 deg. The inlet angle is measured clockwise from the lower tangential and the outlet angle counterclockwise. The calculated results are shown in Figs. 3 and 4, respectively. In Fig. 3, the computed Mach number distribution on blade surface is compared with hodograph solution.[21] The agreement is seen to be quite good. In the procedure of calculation the artificial density coefficient C_0 is chosen to be 0.5. Figure 4 shows the computed Mach number contours. It may be mentioned that the analytical solution for the test case of Figs. 3 and 4 is symmetric. The contour plot of Fig. 4 obtained from the present calculation is not quite symmetric. The nonsymmetry is a result of the use of the artificial density which is nonsymmetric. The second example is for a T_1-(18A6I4b)08 cascade[22] with a 50×11 mesh. The inlet Mach number is 0.832 and the inlet angle is 30 deg. The calculated results are compared with the relaxation solution of Ref. 23. The experimental data of Fig. 5 is taken from Ref. 22.

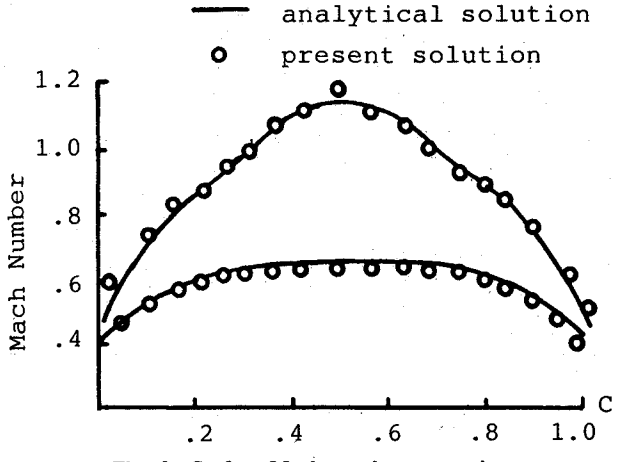

Fig. 3 Surface Mach number comparison.

From Fig. 5, it is seen that the present result along the suction surface is much closer to the experimental data than the result in Ref. 23. The shock position in the present result moves about one to two grids upstream than the real position; this phenomenon is familiar in solutions derived from stream function. The third example is for a DCA 2-8-10 Cascade.[24] The grid points are 50×11, the inlet Mach number is 1.11 and the inlet angle is 62.5 deg. In the present investigation, the shock-capturing method is used to study

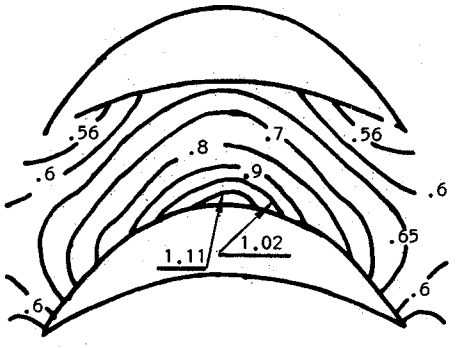

Fig. 4 Mach number contour plot.

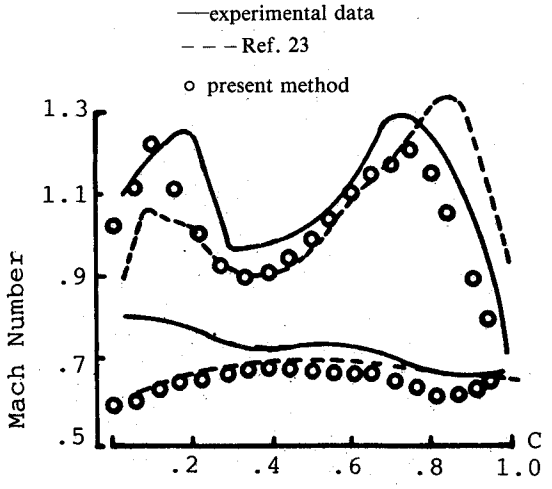

Fig. 5 Mach number distribution around blade.

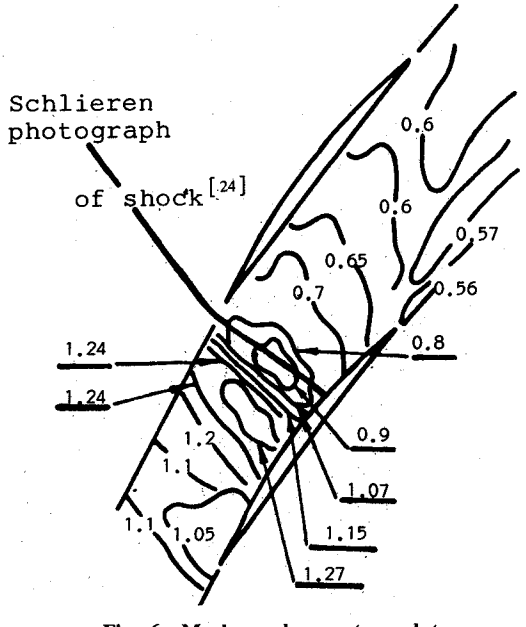

Fig. 6 Mach number contour plot.

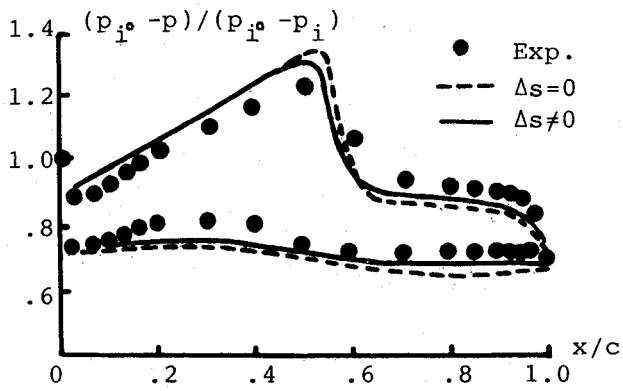

Fig. 7 Convergence history of residual.

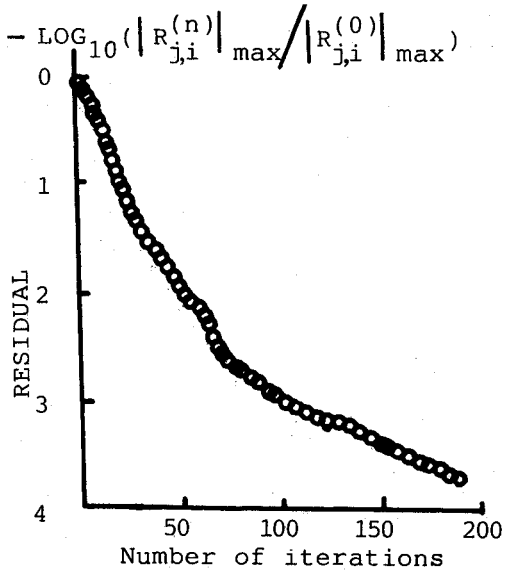

Fig. 8 Pressure distribution on the blade surface (DCA 2-8-10, $Mi = 1.11$).

the same cascade. In Fig. 6, the calculated Mach number contours are compared with the experimental shock position taken from Ref. 24. It can be seen that the computed shock position is slightly upstream of the experimental shock position. Figure 7 shows the convergence-history of residual. It can be seen that if a drop of the residual by three orders of magnitude is taken to be the convergence criterion, convergence, in this case, is achieved in approximately 100 iterations. In the procedure of calculation the coefficient C_0 is chosen 1.5. The density-field distribution for the three examples are reported in Tables 1, 2, and 3 of Ref. 25, respectively.

Finally, it should be pointed out that the effect of entropy increase across the shock has been investigated in example 3 and the result is shown in Fig. 8. It is seen from the figure that the pressure distribution is closer to the experimental data than that without consideration of entropy change.

VIII. Concluding Remarks

Using a combination of artificial compressibility and a new iterative algorithm between the two variables ψ and ρ, a set of Wu's equations governing the fluid flow along the S_1 stream surface is solved. The set of equations consists of a second-order partial differential equation in terms of stream function and a new first-order partial differential equation for density derived from the continuity equation, momentum equation, and Bernoulli's equation. A strongly implicit approximate factorization algorithm of the multidimensional partial differential equations is used in numerical solutions of this set of equations. The problem of nonuniqueness of density in conventional stream function methods is then avoided in the present study.

Acknowledgments

The work reported here was performed under the direct supervision of Prof. Wu Chung-Hua. The author is greatly indebted to him for his valuable advice and encouragement.

References

[1]Hafez, M. M., South, J. C., and Murman, E. M., "Artificial Compressibility Methods for Numerical Solutions of Transonic Full Potential Equations," *AIAA Journal*, Vol. 17, Aug. 1979, pp. 838-844.

[2]Hafez, M. and Lovell, D., "Numerical Solution of Transonic Stream Function Equation," *AIAA Journal*, Vol. 21, March 1983, pp. 327-335.

[3]Bellhaus, W. F., Jameson, A., and Albert, J., "Implicit Approximate-Factorization Schemes for Steady Transonic Flow Problems," *AIAA Journal*, Vol. 16, June 1978.

[4]Holst, T. L. and Ballhaus, W. F., "Fast, Conservative Schemes for the Full Potential Equation Applied to Transonic Flows," *AIAA Journal*, Vol. 17, Feb. 1979.

[5]Holst, T. L., "Implicit Algorithm for the Conservative Transonic Full-Potential Equation Using an Arbitrary Mesh," *AIAA Journal*, Vol. 17, Oct. 1979.

[6]Wang, B.-G. and Wu, C.-H., "Matrix Solution of Compressible Flow on S_1 Stream Surface Through a Turbomachine Blade Row with Splitter Vanes or Tandem Blades," *Journal of Engineering Thermophysics*, Vol. 5, No. 1, 1984, pp. 18-26 (in Chinese).

[7]Baker, T. J., "Potential Flow Calculation by the Approximate Factorization Method," *Journal of Computational Physics*, Vol. 42, 1981, pp. 1-19.

[8]Baker, T. J. and Forsey, C. R., "A Fast Algorithm for the Calculation of Transonic Flow over Wing/Body Combinations," *AIAA Journal*, Vol. 21, Jan. 1983, pp. 60-67.

[9]Roach, R. L. and Sankar, N. L., "The Strongly Implicit Procedure Applied to the Flow of Transonic Turbine Cascades," AIAA Paper 81-0211, 1981.

[10]Habashi, W. G. and Hafez, M. M., "Finite Element Stream Function Solutions for Transonic Turbomachinery Flows," AIAA Paper 82-1268.

[11]Zhao, X., "Solution of Transonic Flow Along S_1 Stream Surface Employing Non-Orthogonal Curvilinear Coordinates and Corresponding Non-Orthogonal Velocity Components," Paper presented at the Conference on Computational Methods in Turbomachinery, The University of Birmingham, April 1984.

[12]Flores, J., Holst, T. L., Kwak, D., and Batiste, D. M., "A New Consistent Spatial Differencing Scheme for the Transonic Full-Potential Equation," *AIAA Journal*, Vol. 22, Aug. 1984, pp. 1027-1034.

[13]Wu, C.-H., "A General Theory of Three-Dimensional Flow in Subsonic and Supersonic Turbomachines of Axial, Radial and Mixed-Flow Types," ASME Paper 50-A-79, Nov. 1952.

[14]Wu, C.-H., "Basic Aerothermodynamic Equations Governing Fluid Flow in Turbomachines Expressed in Terms of Nonorthogonal Curvilinear Coordinates," Research Note, Institute of Mechanics, 1963; and Lecture Notes, China University of Science and Technology, 1975.

[15]Wu, C.-H., "Three-Dimensional Turbomachines Flow Equations Expressed with Respect to Nonorthogonal Curvilinear Coordinates and Methods of Solution," *Proceedings of the 3rd International Symposium of Air-Breathing Engines*, Munich, West Germany, March 1976, pp. 233-252; also *Engineering Thermophysics in China*, Vol. 1, No. 2, Rumford Pub. Co., U.S.A., 1980.

[16]Wu, C.-H. and Wang, B.-G., "Matrix Solution of Compressible Flow on S_1 Surface Through a Turbomachine Blade Row with Splitter Vanes or Tandem Blades," *ASME Journal of Engineering for Gas Turbines and Power*, Vol. 106, April 1984, pp. 449-454.

[17]Wu, C.-H., Wu, W., Hua, Y., and Wang, B.-G., "Transonic Cascade Flow with Given Shock Shape Solved by Separate Subsonic and Supersonic Computations," Paper to be presented at the Conference on Computational Methods in Turbomachinery, The University of Birmingham, England, April 1984, pp. 133-140; see also *Journal of Engineering Thermophysics*, Vol. 5, No. 3, 1984, pp. 256-262 (in Chinese).

[18]Stone, H. L., "Iterative Solution of Implicit Approximations of Multidimensional Partial Differential Equations," *SIAM Journal on Numerical Analysis*, Vol. 5, No. 3, 1968, pp. 530-558.
[19]Wang, B.-G., Hua, Y.-N., Huang, X.-Y., and Wu, C.-H., "Transonic Flow Along Arbitrary Stream Filament of Revolution Solved by Separate Computations with Shock Fitting," Paper 852088, 5th Annual Meeting Chinese Society of Engineering Thermophysics, 1985 (in Chinese); see also ASME Paper 86-GT-30 to be published, June, Germany, 1986.
[20]Wu, C.-H., "Formulas and Tables of Coefficients for Numerical Differentiation with Function Value Given at Unequally Spaced Points and Application to the Solution of Partial Differential Equation," NACA TN 2214, 1950.
[21]Hobson, D. E., "The Hodograph Method for Design on Transonic Turbine Blades," *CUED/A-Turbo/Tr*, Vol. 40, 1972.
[22]Savage, M., Felix, R., and Emery, J., "High-Speed Cascade Tests of a Blade Section Designed for Typical Hub Conditions of High-Flow, Transonic Rotors," NACA RM L55 F07, 1955.
[23]Dodge, P. R., "Transonic Relaxation Methods," ASME 76-GT-63, 1976.
[24]Starken, H., "Untersuchung der Strömung in ebenen Überschall-Verzogerung Gittern," DLR FB 71-99, DFVLR, Institut für Luftstrahlantriebe, 1971 (in German).
[25]Wang, Bao-Guo, "New Iterative Algorithm Between Stream Function and Density for Transonic Cascade Flow," AIAA Paper 85-1594, July 1985.